

Holographic Scattering Amplitudes

C.S. Lam^{1,2,3*}

¹*Department of Physics, McGill University
Montreal, Q.C., Canada H3A 2T8*

²*Department of Physics and Astronomy,
University of British Columbia,
Vancouver, BC, Canada V6T 1Z1*

³*CAS Key Laboratory of Theoretical Physics,
Institute of Theoretical Physics,
Chinese Academy of Sciences,
55 Zhong Guan Cun East Road,
Beijing 100190, China*

Abstract

Inspired by ancient astronomy, we propose a holographic description of perturbative scattering amplitudes, as integrals over a ‘celestial sphere’. Since Lorentz invariance, local interactions, and particle propagations all take place in a four-dimensional space-time, it is not trivial to accommodate them in a lower-dimensional ‘celestial sphere’. The details of this task will be discussed step by step, resulting in the Cachazo-He-Yuan (CHY) and similar scattering amplitudes, thereby providing them with a holographic non-string interpretation.

* Lam@physics.mcgill.ca

I. INTRODUCTION

It is well known that it takes the sum of many Feynman diagrams to produce a scattering amplitude, even in the tree approximation. The discovery of the Parke-Taylor formula [1], giving a one-term expression for any gluon amplitude with all but two identical helicities, prompted much research in the past thirty years to generalize its magic [2] and to obtain compact formulas for other amplitudes. See [3] for a review. In particular, the pioneering work of Witten [4] using twistors of Penrose [5] to interpret amplitudes in a string language has been very influential, giving rise to many expressions of scattering amplitudes as integrals over twistor variables, or over string world-sheet variables [6]. One of the latest is the Cachazo-He-Yuan (CHY) formula for tree amplitudes [7–11], valid in any number of space-time dimensions. Its generalization to one-loop amplitudes has also been attempted [12].

An ordinary string theory contains multiple string excitations, with one of the two world-sheet variables describing length measured along the string. Elementary particles have neither excited states, nor an internal dimension, so it seems odd that the most successful interpretation of the CHY and similar amplitudes to date is via string theories [13, 14]. One obvious reason is the presence of world-sheet complex variables in these formulas, which naturally suggests a string interpretation. In order to avoid it, an alternative explanation for these variables must be found. Inspired by ancient astronomy, we suggest that the complex plane should be interpreted as a Riemann sphere, or rather a ‘celestial sphere’ to make it more physical. With that interpretation, the CHY formula becomes a holographic formula, expressing the scattering amplitude as an integral over the celestial sphere, rather than over configuration space-time variables as in usual quantum field theories. The purpose of this note is to discuss how the CHY and other compact formulas can be arrived at in a step by step manner, starting from the requirement that it should be a holographic theory similar to that of ancient astronomy.

In astronomy, a star appears to be located at the position where its star ray punctures the imaginary celestial sphere, as shown in Fig. 1. In elementary particle scattering, the ‘stars’ and ‘star rays’ can be thought of as being the particle sources/detectors and the particle beams, respectively, and the ‘celestial sphere’ could be taken to be a microscopic imaginary sphere enclosing the interaction region. Being microscopic, uncertainty relation has to be taken into account, which prevents the puncture position to be determined geometrically

like in astronomy. Instead, they must be determined by the surface analogs of Klein-Gordon and Weyl equations of motion (Sec. IIB).

Even with the puncture positions thus determined, there are still many difficulties to overcome for a successful holographic description of the scattering amplitude. First of all, Lorentz invariance must be implemented on the celestial sphere (Sec. IIA). Moreover, particles interact at discrete space-time points, not on a two-dimensional ‘celestial sphere’, and they propagate from one space-time point to another, not on the ‘celestial sphere’. How these could be accommodated on the ‘celestial sphere’ will be discussed in the following sections. On-shell and off-shell tree amplitudes are discussed in Sec. III, spinor helicity amplitudes in Sec. IV, and scalar loop amplitudes in Sec. V. Unlike the string theory where higher genus Riemann surfaces are required to discuss loop amplitudes, making it very difficult beyond one loop, in a field theoretical approach one simply needs to fold up off-shell tree amplitudes in an appropriate manner, whatever the number of loops is. In this way, the off-shell holographic amplitude of Sec. III which possesses *all the correct propagators* can be used to obtain a holographic loop amplitude for any number of loops.

II. ANCIENT ASTRONOMY, HOLOGRAPHY, AND PARTICLE PHYSICS

Astronomy is the world’s oldest science. Long before people could write, observation of celestial phenomena was already an important part of their lives. They knew the correlation between temperature and the seasonal position of the sun, as well as the relation between the height of the tide and the phase of motion. From the unchanging pattern of fixed stars which appeared day after day everywhere on earth, they could have discovered rotational invariance, time translational invariance, as well as a certain amount of spatial translational invariance. In that sense it is the world’s oldest science.

Since naked eyes cannot discern distance to the stars and other celestial objects, they all appear to be painted on a two-dimensional imaginary celestial sphere. See Fig. 1. Astronomy would thus have remained a science of two spatial dimensions if it were not for the motion of Earth, bringing along information in the third dimension. Several hundreds of years ago, people noticed a small seasonal variation of the position of some stars. These variations were attributed to parallax, and to stellar aberrations. Parallax, resulting from the different positions of Earth in different seasons, can be used to measure distance to the stars, thus

providing information in the third dimension. Stellar aberration, coming from the different relative velocity between earth and the star rays in different seasons, shows us how to add velocities that agrees with Galilean invariance. If we were able to measure tiny parallax and stellar aberration even for distant stars, then we could have obtained not only complete three-dimensional spatial information from observations on a two-dimensional celestial sphere, but also all the kinematic invariants including Lorentz invariance.

Even dynamics can be deduced from such two-dimensional observations. Newton's discovery of universal gravitation from Kepler's laws of planetary motion is such an example.

We will refer to any extra information (*e.g.*, third dimension) hidden in the celestial sphere as 'holographic information'. A hologram yields a three-dimensional image because holographic information is stored in the interference patterns of the hologram. Astronomy gives us the correct view of space-time because Earth and planetary motions provide us with holographic information. If particle physics can be described by a holographic theory in two spatial dimensions, then the theory must also contain a sufficient amount of holographic information to yield the correct kinematics and dynamics in our four dimensional space-time.

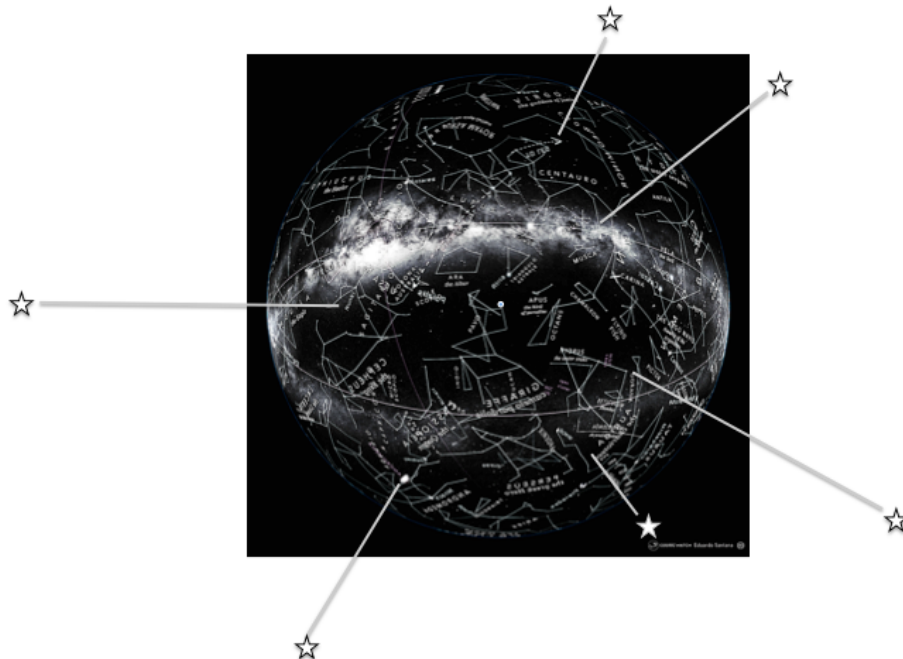


Fig. 1. An imaginary celestial sphere where celestial objects appear to reside. This picture is also valid for particle scattering, if we interpret the stars and star rays to be particle sources/detectors and particle beams, respectively, and the celestial sphere to be an imaginary sphere of microscopic size enclosing the interaction region.

There is a similarity between astronomy and scattering experiments in particle physics which makes a holographic scattering theory of particle physics somewhat plausible. The incoming beams in a scattering experiment are like the star rays, with the particle sources being ‘stars’. Detectors and the outgoing particles are also like stars and star rays, except in reverse. The imaginary ‘celestial sphere’ could be a tiny sphere enclosing the interaction region, though in astronomy we look outward from inside the celestial sphere, and in particle physics we look inward from the outside. This distinction however does bring about an important difference between the two. In astronomy, the star or planetary position σ_i on the celestial sphere is just the puncture of the star ray on the sphere. Its variation with external conditions E (such as time or season) provides the holographic information. With the tiny ‘celestial sphere’ in particle physics, uncertainty relation prevails. The incoming beam is a plane wave much wider than the interaction region, so it is impossible to fix the punctures by geometry. They must be determined by a different means, via a set of *scattering equations*, which come from the surface analogs of the Klein-Gordon and Weyl equations of motion in field theory. Holographic information is provided by external momenta and polarizations.

Even with the punctures thus determined, it is still highly non-trivial to be able to express a scattering amplitude M as a function of E and σ_i . Particle interactions and propagations take place in four-dimensional space-time, not on a two-dimensional celestial sphere. To have a function on the sphere to describe the scattering, this function must implicitly contain vertices and propagators, in such a way to ensure Lorentz invariance. We shall devote the rest of this paper to discuss, step by step, how this can be achieved. As a start, we will review in the next subsection how Lorentz transformation can be implemented on a celestial sphere.

A. Lorentz group representation on a sphere

By a stereographic projection, a sphere can be mapped onto its equatorial plane. The line joining the north pole and a point A on the sphere intersects the equatorial plane at a point B, establishing a correspondence $A \leftrightarrow B$ between the sphere and the plane. The coordinates (x, y) of point B can be represented by a complex number $\sigma = x + iy$, which will also be used to designate the point A as well. No distinction will be made between the sphere and

the complex plane in this note, and a Lorentz transformation on the sphere will simply be specified by the corresponding Lorentz transformation on the plane of complex numbers.

The Lorentz group $SO(3,1)$ is locally equivalent to the $SL(2,C)$ group of 2×2 complex matrices with determinant 1. Such matrices are specified by 3 complex numbers, or six real numbers, which describe the three rotations and three boosts of a Lorentz transformation. More specifically, an $SL(2,C)$ matrix

$$g = \begin{pmatrix} \alpha & \beta \\ \gamma & \delta \end{pmatrix} \quad (\alpha\delta - \beta\gamma = 1)$$

transforms a complex two-dimensional vector (spinor) $\lambda = (\lambda_1, \lambda_2)^T$ into $\lambda' = g\lambda$, and a 2×2 complex matrix

$$P = \sigma_\mu p^\mu = \begin{pmatrix} p^0 + p^3 & p^1 - ip^2 \\ p^1 + ip^2 & p^0 - p^3 \end{pmatrix}$$

into $P' = gPg^T = \sigma_\mu p'^\mu$. Since $\det(P) = p^\mu p_\mu$ and $\det(g) = 1$, this transformation preserves the norm of the four-vector p^μ , showing that $SL(2,C)$ is locally equivalent to the Lorentz group.

The ratio $\sigma = \lambda_1/\lambda_2$ transforms into $\sigma' = (\alpha\sigma + \beta)/(\gamma\sigma + \delta)$. Although the Lorentz group has only a trivial *linear* representation in one dimension, it does have a non-trivial one as shown above when it is represented non-linearly. Hitherto the denominator $(\gamma\sigma + \delta)$ will be denoted by $\xi_g(\sigma)$, or simply $\xi(\sigma)$.

If ψ is a Lorentz spinor or tensor, transforming according to $\psi \rightarrow G\psi$ under a linear Lorentz transformation, then $\psi(\sigma)$ will be called a spinor or tensor *density of weight* w on the sphere if it transforms according to $\psi(\sigma) \rightarrow G\psi(\sigma)\xi(\sigma)^w$. Similarly, $\psi(\boldsymbol{\sigma}) \equiv \psi(\sigma_1, \sigma_2, \dots, \sigma_n)$ will also be called a spinor or tensor density of weight $w = (w_1, w_2, \dots, w_n)$ if $\psi(\sigma_1, \sigma_2, \dots, \sigma_n) \rightarrow G\psi(\sigma_1, \sigma_2, \dots, \sigma_n) \prod_{i=1}^n \xi(\sigma_i)^{w_i}$. In particular, if $w_i = \omega$ for all i , then $\psi(\sigma_1, \sigma_2, \dots, \sigma_n)$ is said to have a *uniform weight* ω . The Lorentz-invariant scattering amplitude M will be obtained by assembling various densities of these types to get a total weight 0.

For later usage, here are some sample weights that can be obtained by a straight forward calculation. $1/\sigma_{ij} \equiv 1/(\sigma_i - \sigma_j)$ has a weight $w = (1, 1)$, and $1/\sigma_\alpha \equiv 1/\prod_{i=1}^n \sigma_{\alpha_i \alpha_{i+1}}$ has a uniform weight $\omega = 2$, where $\alpha = (\alpha_1, \alpha_2, \dots, \alpha_n)$ is a permutation of $(1, 2, \dots, n)$ with $\alpha_{n+1} \equiv \alpha_1$. The differential $d\sigma_i$ has a weight $w_i = -2$.

In the rest of this subsection, the difference between the present holographic approach and that of the AdS₃/CFT₂ correspondence in the literature [15] is explored. These discussions have no bearing on the rest of the article so they can be safely skipped.

The Lorentz group in a (d+1)-dimensional *Minkowskian* space-time is SO(d,1). For a theory possessing scaling and conformal invariance, this symmetry group is enlarged to the conformal group SO(d+1,2). To be conformal, the theory is required not to carry any dimensional parameter such as mass.

There is a mathematical analog in a d-dimensional *Euclidean* space, whose symmetry group is the rotation group SO(d), and its conformal extension is the group SO(d+1,1). In particular, for the celestial sphere or the complex plane with d=2, its conformal group SO(3,1) is the Lorentz group in four-dimensional space-time. It is locally equivalent to SL(2,C), the globally-defined conformal group of the complex plane. However, unlike the Minkowskian conformal group, it allows dimensional parameters such as mass to be present, because the scaling operation in the complex plane, $\sigma \rightarrow \sigma' = \alpha^2 \sigma$, is just a Lorentz boost along the third spatial dimension, where parameters such as mass are not affected.

For physical clarity we prefer to think of SO(3,1) as a Lorentz group of space-time rather than a conformal group of the complex plane. This is where we differ from the AdS₃/CFT₂ approach; anti-deSitter spaces such as AdS₃ never enters into our discussions. There is another reason to regard SO(3,1)~SL(2,C) as a Lorentz group rather than a conformal group, in spite of the fact that we need Lorentz-group representations on the complex plane. If we were to consider it as a conformal group, then the natural objects to study would be the conformal fields, which carry only *abelian* spin quantum numbers. In contrast, in our discussions, we need (non-abelian) spinors and vectors in four-dimensional space-time, in the form as Lorentz densities on the sphere.

B. Holographic scattering amplitude

By an n -particle holographic scattering amplitude, we mean an amplitude that can be expressed as an integral over the ‘celestial sphere’,

$$M = \int d\sigma_1 d\sigma_2 \cdots d\sigma_n A(E, \sigma_1, \sigma_2, \cdots, \sigma_n) := \int d^n \boldsymbol{\sigma} A(E, \boldsymbol{\sigma}), \quad (1)$$

where E provides external input such as momentum and polarization of the scattering particles. The puncture positions σ_i on the sphere are determined by a set of $(n+x)$ *scattering*

equations of the form $\phi_i(E, \boldsymbol{\sigma}, \boldsymbol{\tau}) = 0$, where $\boldsymbol{\tau} = (\tau_1, \dots, \tau_m)$ are extra auxiliary variables that may or may not be present. In the simplest case to be discussed in the next section, the auxiliary variables are absent, and $x = 0$, so there are just enough scattering equations to determine all the puncture positions σ_i . In general, we may use a set of δ -functions to implement the scattering equation constraints, so that

$$A(E, \boldsymbol{\sigma}) = \int d^m \boldsymbol{\tau} \left[\prod_{i=1}^{n+x} \delta(\phi_i(E, \boldsymbol{\sigma}, \boldsymbol{\tau})) \right] B(E, \boldsymbol{\sigma}, \boldsymbol{\tau}), \quad (2)$$

where B contains the dynamics in such a way that M remains Lorentz invariant.

The form and the number of scattering equations $\phi_i = 0$ depend on whether the external inputs E are just the momenta k_i of the scattering particles, or momenta k_i plus polarizations ϵ_i in the spinor-helicity form. We will study these two cases separately.

III. MOMENTUM INPUT ALONE

In that case, suppose σ_i is the puncture made by the incoming beam with momentum k_i on the ‘celestial sphere’. Then it is convenient to construct a vector density $k(\sigma) = \sum_{i=1}^n k_i / (\sigma - \sigma_i)$ to summarize these inputs. This density vanishes in the absence of external momenta, satisfies the source equation $\bar{\partial} k(\sigma) = 2\pi i \sum_{i=1}^n k_i \delta^2(\sigma - \sigma_i)$, and is a vector density of weight 2 as shown below, provided momentum is conserved. Under a Lorentz transformation discussed in Sec. IIA, it transforms as

$$k(\sigma) \rightarrow \sum_{i=1}^n \frac{k_i}{\sigma - \sigma_i} \xi(\sigma) \xi(\sigma_i) = \sum_{i=1}^n \frac{k_i}{\sigma - \sigma_i} \xi(\sigma) [\xi(\sigma) - \gamma(\sigma - \sigma_i)] = \xi(\sigma)^2 k(\sigma). \quad (3)$$

The second term within the square bracket vanishes on account of momentum conservation. Hence it has weight 2.

A. Massless momenta

If all the incoming momenta are massless, $k_i^2 = 0$, we also require $k(\sigma)^2 = 0$ to be true for all $\sigma \neq \sigma_i$. This requirement on the sphere is the counterpart of the Klein-Gordon equation $\partial^2 \phi(x) = 0$ for a massless field in space-time. With

$$k(\sigma) \cdot k(\sigma) = \sum_{i \neq j} \frac{k_i \cdot k_j}{(\sigma - \sigma_i)(\sigma - \sigma_j)} = \sum_i \frac{1}{\sigma - \sigma_i} \sum_{j \neq i} \frac{2k_i \cdot k_j}{\sigma_i - \sigma_j} = 0$$

for all σ , it implies

$$f_i(\boldsymbol{\sigma}) \equiv \sum_{j \neq i} \frac{2k_i \cdot k_j}{\sigma_{ij}} = 0, \quad \text{for } 1 \leq i \leq n, \quad (4)$$

which is the CHY scattering equation [7]. By a calculation similar to (3), one can also show that $f_i(\boldsymbol{\sigma})$ is a scalar density of weight $w_k = 2\delta_{ki}$ if momentum is conserved.

Unlike astronomy, where each star ray fixes a single puncture, here each set of initial momenta gives rise to $(n-3)!$ sets of puncture positions because that is how many solutions the CHY scattering equations yield [7]. The δ -function in (2) implies a sum over all these sets of positions. In astronomy, it is the earth's motion that provides holographic information about the third spatial dimension. Here, it is the values of $k_i \cdot k_j$ that provides the holographic information, not only for a third spatial dimension, but in principle for any number of extra spatial (and temporal) dimensions.

B. Off-shell and/or massive momenta

Eq. (4) needs to be modified for massive particles, and/or off-shell external lines. This can be accomplished by adding a term in the numerator of the scattering equation to modify it to

$$\hat{f}_i(\boldsymbol{\sigma}) \equiv \sum_{j \neq i} \frac{2k_i \cdot k_j + \mu_{ij}}{\sigma_{ij}} = 0, \quad (5)$$

with a suitably chosen set of parameters $\mu_{ij} = \mu_{ji}$ ($j \neq i$).

In order to have a smooth transition back to the massless on-shell limit, and in order for the off-shell amplitude to be Lorentz invariant, we need to keep $\hat{f}_i(\boldsymbol{\sigma})$ a scalar density with the same weight $w_k = 2\delta_{ki}$. This requires $\sum_{j \neq i} (2k_i \cdot k_j + \mu_{ij}) = 0$, or equivalently,

$$\sum_{j \neq i} \mu_{ij} = 2k_i^2, \quad 1 \leq i \leq n, \quad (6)$$

where k_i^2 is the off-shell amount of the external momentum k_i . There are many possible solutions to this requirement, as there are $n(n-1)/2$ unknowns μ_{ij} ($i \neq j$) and only n constraints from the weight requirement. For example, if $k_+^2 = k_-^2 = q^2$ and all other $k_i^2 = 0$, then one solution of (6) is $\mu_{+-} = 2q^2$ with all other $\mu_{ij} = 0$ [16]. Another possibility is $\mu_{ij} = -2\kappa_i \cdot \kappa_j$, where κ_i are d -dimensional vectors satisfying momentum conservation such that $\kappa_i^2 = k_i^2$ [17, 18].

However, if we also demand the resulting amplitude to be the same as that given by the sum of *all* off-shell planar Feynman tree diagrams, then the solution of $\mu_{ij} = \mu_{ji}$ ($i \neq j$) for particles of mass $m \geq 0$ is uniquely given by [19]

$$\mu_{i,i\pm 1} = k_i^2 + k_{i\pm 1}^2 - m^2, \quad (7)$$

$$\mu_{i,i\pm 2} = -k_{i\pm 1}^2 + m^2, \quad (8)$$

$$\mu_{i,i\pm p} = 0, \quad (\text{if } 2 < p \leq n). \quad (9)$$

These equations should be interpreted in the following way. Being a planar diagram, the momentum carried by every propagator is equal to the sum of a set of consecutive external lines. Plus signs in the subscripts correspond to clockwise counting, mod n , and minus signs correspond to counter-clockwise counting. Eq. (7) applies to two neighbouring lines, (8) to two next neighbouring lines, and (9) to two lines with a gap of 2 or more.

For a given pair (i, j) , we get different results μ_{ij} from (7) to (9) depending on whether we reach j from i clockwise or counter-clockwise. The true answer should be the sum of the two. This completes the explanation of Eqs. (7) to (9).

These equations are derived using the fact that if S is a contiguous set of neighbouring lines, then [19]

$$\sum_{i,j \in S, i < j} \mu_{ij} = \sum_{i \in S} k_i^2 - m^2 \quad (10)$$

must be satisfied in order for a propagator $1/((\sum_{i \in S} k_i)^2 - m^2)$ to be contained in the amplitude. If the holographic amplitude contains *all* Feynman diagrams, then a propagator is present in the amplitude for *every* consecutive set S . In this way one arrives at (7) to (9) after some algebra.

If the amplitude corresponds to a *single* Feynman diagram, but not the sum of *all* of them, then (10) needs to be satisfied only for those sets S which give rise to a propagator in that particular Feynman diagram, but not all possible sets S . This calls for many fewer conditions and the solution for μ_{ij} is no longer unique. While (7) to (9) always give a valid solution, there are other ones as well.

There is an exception when $n = 4$. This is so because a Feynman tree diagram contains $(n-3)$ propagators. The momentum carried by a propagator, up to a sign, is equal to the sum of all the external momenta on one side of the propagator, and is also equal to the sum of all the external momenta on the other side of the propagator. In order for this propagator

to be present, there are *two* sets of condition (10) to be satisfied, one on either side of the propagator. With $(n-3)$ propagators, there are $2(n-3)$ requirements. On top of these, μ_{ij} must also satisfy (6) in order for \hat{f}_i to have the correct weights, so altogether, there are $2(n-3) + n = 3n - 6$ conditions to be obeyed by $n(n-2)/2$ unknowns μ_{ij} . For $n = 4$, the two numbers are equal, which means that the set of μ_{ij} giving rise to a *single* Feynman diagram is unique, and therefore it must be identical to those in (9) to (10). Already for $n = 5$, there are 10 independent μ_{ij} but only 9 conditions, so the solution is no longer unique.

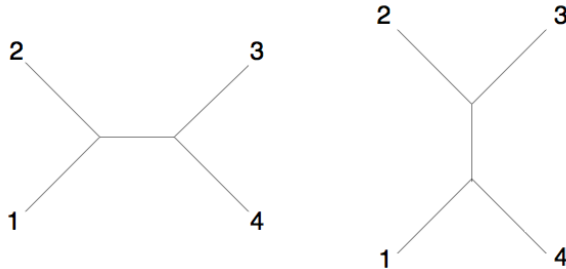


Fig. 2. The s -channel (left) and the t -channel (right) contributions to a four-point planar amplitude with cyclic order (1234) for its external lines.

As an illustration, let us use (10) to obtain directly the unique solution for $n = 4$ from *one* Feynman diagram. According to (10), to produce the propagator in the s -channel diagram in Fig. 2, we need to have

$$\mu_{12} = k_1^2 + k_2^2 - m^2, \quad \mu_{34} = k_3^2 + k_4^2 - m^2. \quad (11)$$

Together with (6), these six equations can be used to solve for the six μ_{ij} , yielding, other than (11), also

$$\begin{aligned} \mu_{13} &= -k_2^2 - k_4^2 + 2m^2, & \mu_{14} &= k_1^2 + k_4^2 - m^2, \\ \mu_{23} &= k_2^2 + k_3^2 - m^2, & \mu_{24} &= -k_3^2 - k_1^2 + 2m^2. \end{aligned} \quad (12)$$

They agree with the rules given in (7) to (9), and they also automatically contain the t -channel propagator condition in the second and the third equations of (12).

C. Holographic tree amplitude

With momentum input alone, the on-shell ($m = 0$, $k_i^2 = 0$) scattering equation $\phi_i = f_i(E, \boldsymbol{\sigma})$ contains no auxiliary variable $\boldsymbol{\tau}$, so there are no $\boldsymbol{\tau}$ -integrations in (2). Moreover,

via a suitable Lorentz transformation (which contains three arbitrary complex numbers), one can fix any three punctures $\sigma_p, \sigma_q, \sigma_r$ to take on any value. In this way the number of σ -integrations can be reduced from n to $n-3$. Correspondingly, it can be shown (see the remark below eq. (15)) that only $(n-3)$ f_i 's are linearly independent, so they can be used to determine the remaining $(n-3)$ puncture positions σ_i . As a result, (1), (2) can now be replaced by

$$M_n = \int \left(\prod_{i \neq p, q, r} d\sigma_i \delta(f_i) \right) \sigma_{pqr}^2 C_n(E, \sigma_1, \sigma_2, \dots, \sigma_n) := \int d\bar{\Omega}_{pqr} C_n(E, \boldsymbol{\sigma}). \quad (13)$$

The weight of each $\delta(f_i)$ and each $d\sigma_i$ is -2 when $i \neq p, q, r$, so for convenience the quantity $\sigma_{pqr} := \sigma_{pq}\sigma_{qr}\sigma_{rp}$ has been introduced to give $d\bar{\Omega}_{pqr}$ a uniform weight of $\omega = -4$. As a result, M is Lorentz invariant if $C_n(E, \boldsymbol{\sigma})$ has a uniform weight $\omega = +4$. Different choice of C_n corresponds to different dynamics, but it turns out that its σ -dependence always consists of products of $1/\sigma_{ij}$'s as these are the fundamental σ -quantities containing fixed weights.

Because of that it is often useful to convert (13) into a complex-integration form

$$M_n = \int_{\mathcal{O}} \left(\prod_{i \neq p, q, r} d\sigma_i \frac{1}{(2\pi i) f_i} \right) \sigma_{pqr}^2 C_n(E, \sigma_1, \sigma_2, \dots, \sigma_n) := \int_{\mathcal{O}} d\Omega_{pqr} C_n(E, \boldsymbol{\sigma}), \quad (14)$$

with \mathcal{O} being the contour surrounding every $f_i = 0$ counter-clockwise. This form is useful because zeros of f_i needed to evaluate (13) are determined by polynomials of degree $(n-3)!$ [7], which are difficult to obtain beyond $n = 4$. In contrast, in the form of (14), one can distort the contour away from $f_i = 0$ to enclose poles of C_n in σ_i , to allow residue calculus to be used on these explicit poles to evaluate M_n .

D. Propagator

Whatever the dynamics, an n -point tree diagram with cubic vertices contains $(n-3)$ propagators, which is also the number of f_i 's in (14). That is not an accident, because it turns out that each integration turns a $1/f_i$ into a propagator. In this way the $(n-3)$ propagators in the Feynman diagram are built up from the $(n-3)$ f_i 's present, through the $(n-3)$ integrations in (14). Which f_i turns into which propagator in which Feynman diagram depends completely on the poles of C_n around which the integral is evaluated.

The denominator of a propagator in a planar Feynman diagram is given by $(k^S)^2 := \left(\sum_{j \in S} k_j \right)^2$ for some consecutive set S of external lines. Since the scattering function f_i

depends both on $k_i \cdot k_l$ as well as σ_{il} , it seems somewhat miraculous that after evaluation at the poles of C_n , whatever they are, the σ_{il} 's would always take on values that turn f_i into $(k^S)^2$. This miracle occurs because of the following sum rule.

For every $i \in S$, define a set of *partial scattering functions* by

$$f_i^S = \sum_{j \in S, j \neq i} \frac{2k_i \cdot k_j}{\sigma_{ij}}.$$

If S is the set of all lines $A = \{1, 2, 3, \dots, n\}$, then f_i^S is the scattering function f_i in (4). Otherwise, it consists of some but not all the terms in f_i .

By a straight-forward calculation, it can be shown that [20]

$$\begin{aligned} \sum_{i \in S} f_i^S &= 0, \\ \sum_{i \in S} f_i^S \sigma_i &= (k^S)^2 := \left(\sum_{i \in S} k_i \right)^2, \\ \sum_{i \in S} f_i^S \sigma_i^2 &= 2k^S \cdot \sum_{i \in S} k_i \sigma_i. \end{aligned} \tag{15}$$

In particular, if $S = A$, momentum conservation shows that only $(n-3)$ f_i 's are linearly independent, as previously claimed. Also, if every $f_i^S = 0$ except $i = t$ and p , then the first two sum rules imply

$$f_t^S = -f_p^S = \frac{(k^S)^2}{\sigma_{tp}}. \tag{16}$$

It is through (16) that f_t morphs into the inverse propagator $(k^S)^2$, in a way outlined in the following sketch. For a more detailed explanation please see [20].

We will call an external line y 'non-integrating' if the factor $1/f_y$ is absent in the integral (14). Initially the constant lines p, q, r are the non-integrating lines. Let S be a set of external lines containing one and only one non-integrating line p , and m other lines i , in such a way that in the limit $\sigma_{ip} = O(\epsilon) \rightarrow 0 \forall i \in S$, C_n behaves like $1/\epsilon^{2m}$. Now pick any line $t \neq p$ within the set, distort the contour \mathcal{O} in (14) away from $f_t = 0$ to enclose the ϵ -pole of C_n , but keeping it surrounding the rest of the zeros of f_i as before. With $C_n \sim 1/\epsilon^{2m}$, the integrand of (14) would contain a simple pole in ϵ . The integration $\int d\epsilon$ around $\epsilon = 0$ would factorize M into two parts, one containing the lines in S , and the other the lines in its complement \bar{S} . With the help of (16), $1/f_t$ would turn into the propagator $1/(k^S)^2$, linking these two parts.

We can repeat this procedure to expose more propagators in S and \bar{S} . Each of these two sets contains two non-integrating lines to choose from, q, r in \bar{S} and p, t in S . Line t has now become a non-integrating line because $1/f_t$ has been morphed away to become a propagator so it is no longer present. Note also that after the integration, every σ_{ij} for $i \in S$ and $j \in \bar{S}$ becomes σ_{pj} because every $\sigma_{ip} = O(\epsilon) \rightarrow 0$.

This procedure can be repeated over and over again until all the $(n-3)$ propagators are exposed. There are many ways of doing it depending on the order the different propagators are exposed, but the end result yields the same Feynman diagram.

Propagators reflect the time-energy uncertainty condition. In ordinary quantum field theories, (the denominator of) a propagator $(1/\partial^2)\delta^4(x)$ emerges from the Klein-Gordon equation of motion $\partial^2\phi(x) = 0$ when a particle goes off-shell, with the factor $\delta^4(x)$ coming directly from canonical quantization. It is the same propagator whatever the interactions are. Things are very similar in a holographic scattering theory. The propagator $1/f_t$ comes from the scattering equation $f_t = 0$ when the contour is distorted away from this ‘on-shell’ value to enclose the poles of C_n . Again its presence is independent of the dynamics. This suggests that quantization is somehow related to this contour manipulation of the holomorphic scattering function, though it is not yet clear in exactly what way.

So far we have concentrated on the on-shell massless amplitudes. For $m \neq 0$ and/or $k_i^2 \neq 0$, correct propagators will also emerge in the same way because it is this requirement that determines μ_{ij} in eq. (5). The expressions (13) and (14) for the scattering amplitude also remain the same if f_i is replaced by \hat{f}_i .

E. Dynamics

In perturbative quantum field theories, dynamics is specified by the vertex. This is also the case in a holographic scattering theory.

The n -point holographic amplitude given by (14) contains only $(n-3)$ integrations. In particular, for $n = 3$, there is no integration at all so the vertex is given simply by $M_3 = \sigma_{pq}^2 C_3(E, \sigma_p, \sigma_q, \sigma_r)$. This is why it is natural to have cubic interactions in holographic theories. To some extent it is simply a consequence of demanding Lorentz invariance on the ‘celestial sphere’.

In what follows we shall concentrate on the scalar ϕ^3 theory and the pure Yang-Mills

theory, though other theories can be similarly analyzed.

The vertex of a ϕ^3 theory is simply the coupling constant. For simplicity we shall take it to be 1, hence $C_3(E, \sigma_1, \sigma_2, \sigma_3) = 1/\sigma_{123}^2$. Similarly, other than the color factor, C_3 for the Yang-Mills theory can be obtained from the triple gluon vertex to be $C_3(E, \sigma_1, \sigma_2, \sigma_3) = [(\epsilon_1 \cdot \epsilon_2)(\epsilon_3 \cdot k_1) + (\epsilon_2 \cdot \epsilon_3)(\epsilon_1 \cdot k_2) + (\epsilon_3 \cdot \epsilon_1)(\epsilon_2 \cdot k_3)]/\sigma_{123}^2$. In both cases C_3 has a uniform weight of $\omega = +4$ which renders the scattering amplitude M Lorentz invariant.

Locality in usual quantum field theory is implemented by demanding contact interactions in space-time. In a holographic theory without an explicit third spatial dimension, this requirement is replaced by the absence of a form factor in the three-point interaction C_3 . In principle, one can multiply the above results by a function of $k_i \cdot k_j$ without changing its Lorentz weight, but that would be introducing a form factor corresponding to non-local interactions. Similar remarks also apply to C_n for $n > 3$.

To obtain the holographic tree amplitude with the specified dynamics, C_n must be chosen to yield the correct Feynman n -point tree diagrams. In other words, each non-zero contribution to (1) must contain $n-3$ propagators joining the proper vertices.

Let $\alpha = (\alpha_1 \alpha_2 \alpha_3 \cdots \alpha_n)$ be a permutation of $(123 \cdots n)$. Then

$$\sigma_\alpha := \sigma_{\alpha_1 \alpha_2} \sigma_{\alpha_2 \alpha_3} \cdots \sigma_{\alpha_{n-1} \alpha_n} \sigma_{\alpha_n \alpha_1}$$

has a uniform weight -2 for every α . Since C_n must have a uniform weight of $+4$, the obvious choice in the case of a scalar theory is $C_n = 1/(\sigma_\alpha \sigma_\beta)$, where β is another permutation of $123 \cdots n$ which may or may not be the same as α . With this choice, M_n is just the color-stripped amplitude of the CHY bi-adjoint scalar theory [9]. When $\beta = \alpha$, M_n is given by the sum of all planar tree diagrams whose external lines are ordered according to α . For $\beta \neq \alpha$, only some of these diagrams are summed.

Putting these together, we arrive at the CHY formula for color-stripped scalar amplitude for massless on-shell particles. In the case $\beta = \alpha = (123 \cdots n)$, it is

$$M_n = \int \left(\prod_{i \neq p, q, r} d\sigma_i \delta(f_i) \right) \frac{\sigma_{pqr}^2}{(\sigma_{12} \sigma_{23} \cdots \sigma_{n-1, n} \sigma_{n1})^2}. \quad (17)$$

It is known that this amplitude is independent of the choice of p, q, r [7, 9]. For massive and/or off-shell particles, we merely have to replace f_i in (17) by \hat{f}_i of (5).

There are other possible choices for C_n that carry the same Lorentz weight $+4$. For example, we may multiply C_n of the last paragraph by a function of $k_i \cdot k_j$. This however

introduces a form factor which makes the theory non-local. We could also multiply C_n in the last paragraph by a cross ratios $\sigma_{ij}\sigma_{kl}/\sigma_{ik}\sigma_{jl}$, or a function of that, but then we will not get the right propagators because the zeros and the poles present in the cross ratio would ruin the $1/\epsilon^{2m}$ behaviour of C_n . This is illustrated in the following example.

The two Feynman planar diagrams shown in Fig. 3 are the same, but drawn differently so that the external lines on the left are ordered according to $\alpha = (123456789)$, and on the right according to $\beta = (124395786)$. The amplitude is given by (14) with $C_n = 1/(\sigma_\alpha\sigma_\beta)$. We will first review how this choice of α and β in (14) leads to the Feynman diagram in Fig. 3, then we will show how the presence of an additional cross ratio ruins it.

The propagators labelled a to f are produced according to the discussions after (16). In this illustration, we shall take the constant lines to be $p, q, r = 2, 4, 6$, and the propagators to be exposed in the order a, b, c, d, e, f . With the non-integrating lines underlined, and a cap on top of the line t that morphs into a propagator at every step, the relevant sets S that gives rise to these propagators by having $C_n \sim 1/\epsilon^{2m}$ are

$$S_\alpha^a = \{\hat{1}\underline{2}\}, S_\beta^a = \{\hat{1}\underline{2}\}; \quad S_\alpha^b = \{\hat{3}\underline{4}\}, S_\beta^b = \{\hat{4}\underline{3}\}; \quad S_\alpha^c = \{\underline{5}\hat{6}\hat{7}\hat{8}\hat{9}\}, S_\beta^c = \{\hat{9}\hat{5}\hat{7}\hat{8}\hat{6}\};$$

$$S_\alpha^d = \{\hat{5}\hat{6}\hat{7}\hat{8}\}, S_\beta^d = \{\hat{5}\hat{7}\hat{8}\hat{6}\}; \quad S_\alpha^e = \{\underline{6}\hat{7}\hat{8}\}, S_\beta^e = \{\hat{7}\hat{8}\hat{6}\}; \quad S_\alpha^f = \{\hat{7}\underline{8}\}, S_\beta^f = \{\hat{7}\underline{8}\}.$$

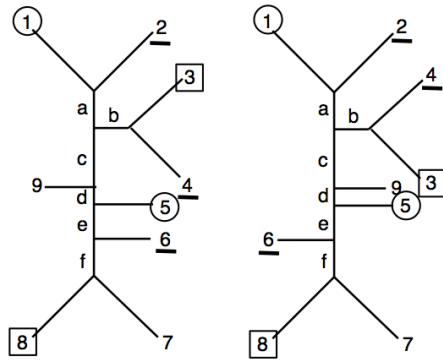


Fig. 3. Two equivalent Feynman diagrams, one showing the α -ordering and the other the β -ordering. The six propagators are labelled a, b, c, d, e, f , and the three constant lines p, q, r in (14) are chosen in this illustration to be $2, 4, 6$, shown underlined in the diagrams. Lines $i, j = 1, 5$ in the cross ratio $R = \sigma_{ij}\sigma_{kl}/\sigma_{ik}\sigma_{jl}$ are marked with a circle, and $k, l = 3, 8$ are marked with a square.

Now insert the cross ratio $R = (\sigma_{15}\sigma_{38})/(\sigma_{13}\sigma_{58})$ so that $C_n = R/(\sigma_\alpha\sigma_\beta)$. In Fig. 3, a circle is put on the lines $i, j = 1, 5$ and a square is put on the lines $k, l = 3, 8$. How the cross

ratio changes after each integration is shown below, using the fact that every σ_{ij} for $i \in S$ and $j \in \bar{S}$ becomes σ_{pj} after the ϵ -integration:

$$R = \frac{\sigma_{15}\sigma_{38}}{\sigma_{13}\sigma_{58}} \xrightarrow{a} \frac{\sigma_{25}\sigma_{38}}{\sigma_{23}\sigma_{58}} \xrightarrow{b} \frac{\sigma_{25}\sigma_{48}}{\sigma_{24}\sigma_{58}} \xrightarrow{c} \frac{\sigma_{25}\sigma_{48}}{\sigma_{24}\sigma_{58}} \xrightarrow{d} \frac{\sigma_{26}\sigma_{48}}{\sigma_{24}\sigma_{68}} \xrightarrow{e} \frac{\sigma_{26}\sigma_{46}}{\sigma_{24}\epsilon}. \quad (18)$$

When we try to pull out the propagators a, b, c, d successively, R just rides along and changes its value after each integration. However, when we try to pull out the next propagator e , there is an additional $1/\epsilon$ present so that C_n now behaves like $1/\epsilon^{2m+1}$ ($m = 2$) rather than $1/\epsilon^{2m}$. As a result, the ϵ -pole in (14) at this stage becomes a double pole, not a simple pole anymore, so the result of the integration is something much more complicated than a simple propagator e . The introduction of R into C_n therefore ruins factorization and the end result is no longer a Feynman diagram.

In the case of Yang-Mills, the generalization of C_3 to C_n is the reduced Pfaffian given in [8, 9, 21]. The resulting amplitude is cyclically invariant and gauge invariant, factorizes as in field theory, has no form factor, and has a uniform weight of +4 as required. Under these requirements this reduced Pfaffian form is likely to be unique, but I know of no general proof of that.

IV. SPINOR HELICITY TREE AMPLITUDE

With momentum input, the dynamical factor $C_n(E, \boldsymbol{\sigma})$ in a Yang-Mills theory is proportional to a rather complicated object known as reduced Pfaffian [8, 9]. If polarization is also added to the input E , then the resulting dynamical factor turns out to be much simpler.

This is accomplished by using the spinor helicity technique, whose salient feature will be reviewed in the following subsection. This input changes the scattering equations, and the construction of the scattering amplitude.

A. Spinor helicity technique

This technique makes use of the local equivalence between $\text{SO}(3,1)$ and $\text{SU}(2) \times \text{SU}(2)$, to represent a light-like Lorentz four-vector $q^\mu \in \text{SO}(3,1)$ by a product of two spinors λ and

$\tilde{\lambda} \in \text{SU}(2) \times \text{SU}(2)$:

$$(\sigma_\mu q^\mu)_{a\dot{a}} = q_{a\dot{a}} = \begin{pmatrix} q^0 + q^3 & q^1 - iq^2 \\ q^1 + iq^2 & q^0 - q^3 \end{pmatrix} = \lambda_a \tilde{\lambda}_{\dot{a}}. \quad (19)$$

In particular, the momentum k_i of the i th massless gluon can be expressed as $\lambda_i \tilde{\lambda}_i$, and a dot product of two vectors can be written as multiplication of two spinor products,

$$2k_i \cdot k_j = (\epsilon_{ab} \lambda_i^a \lambda_j^b) (\epsilon_{\dot{a}\dot{b}} \tilde{\lambda}_i^{\dot{b}} \tilde{\lambda}_j^{\dot{a}}) \equiv \langle ij \rangle [ji].$$

Note that $\epsilon_{ab} = -\epsilon_{ba}$ so $\langle ij \rangle = -\langle ji \rangle$ and $\langle ii \rangle = 0$. Similarly $[ij] = -[ji]$.

The polarization vector ϵ_i^\pm satisfies $\epsilon_i^\pm \cdot \epsilon_i^\pm = 0$ so (19) can again be used to write it as

$$\begin{aligned} (\epsilon_i^-)_{a\dot{a}} &= \sqrt{2} \frac{\lambda_i^a \tilde{\mu}^{\dot{a}}}{[\tilde{\lambda} \tilde{\mu}]}, \\ (\epsilon_i^+)_{a\dot{a}} &= \sqrt{2} \frac{\mu^a \tilde{\lambda}_i^{\dot{a}}}{\langle \mu \lambda \rangle}, \end{aligned} \quad (20)$$

where the normalization is chosen so that $\epsilon_i^- \cdot \epsilon_i^+ = -1$, and gauge dependence is specified by the arbitrary spinors μ and $\tilde{\mu}$. The spinor-helicity expression for a Lorentz-invariant scattering amplitude M is obtained by making these substitutions to express it as spinor products of λ_i 's and $\tilde{\lambda}_i$'s.

It is important to note that k_i^μ does not determine λ_i and $\tilde{\lambda}_i$ uniquely, for an arbitrary scaling $\lambda_i \rightarrow s_i \lambda_i$ and $\tilde{\lambda}_i \rightarrow \tilde{\lambda}_i / s_i \equiv \tilde{s}_i \tilde{\lambda}_i$ leaves k_i^μ unchanged. Under such a scaling, $\epsilon_i^- \rightarrow s_i^2 \epsilon_i^-$ and $\epsilon_i^+ \rightarrow \tilde{s}_i^2 \epsilon_i^+$. If \mathcal{N} denotes the set of negative-helicity gluons and \mathcal{P} the set of positive-helicity lines in a gluon amplitude, the fact that a gluon amplitude M should be linear in each of the polarization vectors tells us that M should scale like

$$M \rightarrow \left(\prod_{n \in \mathcal{N}} s_n^2 \prod_{p \in \mathcal{P}} \tilde{s}_p^2 \right) M. \quad (21)$$

This relation constrains the number of λ_i 's and $\tilde{\lambda}_i$'s allowed in the numerator and the denominator of M . If m_n is the number of λ_n in the numerator, minus the number in the denominator, plus the number of $\tilde{\lambda}_n$ in the denominator, minus that number in the numerator, then according to (21) we should have $m_n = +2$ for every $n \in \mathcal{N}$. Similarly, if m_p is the number of $\tilde{\lambda}_p$ in the numerator, minus the number in the denominator, plus the number of λ_p in the denominator, minus that number in the numerator, then $m_p = -2$ for every $p \in \mathcal{P}$.

There is another constraint coming from the energy dimension of M , which should be $4 - n$, in the unit when the energy dimension of k is taken to be 1 and that of λ and $\tilde{\lambda}$ is taken to be $\frac{1}{2}$. As a result, the total number of spinor products $\langle ij \rangle$ and $[ij]$ in the numerator minus those in the denominator should be $4 - n$.

These constraints are nicely illustrated in the Parke-Taylor formula for the scattering amplitude with $(n-2)$ positive-helicity gluons and 2 negative-helicity gluons residing in lines i and j [1]:

$$M = \frac{\langle ij \rangle^4}{\langle 12 \rangle \langle 23 \rangle \cdots \langle n-1, n \rangle \langle n1 \rangle}. \quad (22)$$

The total number of spinor products in the numerator minus those in the denominator is indeed $4 - n$. Moreover, $m_n = +2$ and $m_p = -2$ are also clearly displayed.

B. Spinor scattering equations

The scattering equations discussed in the last section are constructed via a vector density $k(\sigma)$ sourced by the input momenta k_i . In a similar way, when both k_i and ϵ_i are provided as inputs in the spinor helicity form, we could likewise construct smooth spinor densities $\lambda(\sigma)$ and $\tilde{\lambda}(\sigma)$, sourced by the external spinors, to summarize the input. From (20), we see that negative-helicity gluons provide only for λ_n , not the tilde spinor which is a gauge artifact, and positive-helicity gluons provide only for $\tilde{\lambda}_p$, not the un-tilde spinor which is also a gauge artifact. Furthermore, these spinors are uncertain up to a scaling factor t_n and \tilde{t}_p respectively. Thus the only input that can source a *smooth* $\lambda(\sigma)$ is $t_n \lambda_n$, for some suitable scales t_n , and the only input that can source a smooth $\tilde{\lambda}(\sigma)$ is $\tilde{t}_p \tilde{\lambda}_p$, for some suitable scales \tilde{t}_p . If we double the scaling factors in all the sources, $\lambda(\sigma)$ and $\tilde{\lambda}(\sigma)$ will remain smooth, but their values must be doubled as well. To prevent the spinor density $\lambda(\sigma)$ to be affected by such a scaling, we should take out from it a smooth scaling factor $t(\sigma)$, and similarly a scaling factor $\tilde{t}(\sigma)$ from the spinor density $\tilde{\lambda}(\sigma)$. Hence the relevant densities sourced by the known spinor helicity inputs should be

$$\begin{aligned} t(\sigma)\lambda(\sigma) &= \sum_{n \in \mathcal{N}} \frac{t_n \lambda_n}{\sigma - \sigma_n}, \\ \tilde{t}(\sigma)\tilde{\lambda}(\sigma) &= \sum_{p \in \mathcal{P}} \frac{\tilde{t}_p \tilde{\lambda}_p}{\sigma - \sigma_p}. \end{aligned} \quad (23)$$

Since $k_i = \lambda_i \tilde{\lambda}_i$ for all i , it is natural to require $k(\sigma) = \lambda(\sigma) \tilde{\lambda}(\sigma)$ for all σ . This requirement, written in the form $\lambda(\sigma) k(\sigma) = \lambda(\sigma) (\sigma_\mu k^\mu(\sigma)) = 0$, is simply the Weyl equation of motion for a spinor. It is the counterpart of the Klein-Gordon equation $k_\mu(\sigma) k^\mu(\sigma) = 0$ for scalars on the ‘celestial sphere’.

With this requirement, it is straight forward to show that [22] the following scattering equations must be satisfied:

$$\begin{aligned} t_p \lambda_p &= \sum_{n \in \mathcal{N}} \frac{t_n \lambda_n}{\sigma_p - \sigma_n}, & (p \in \mathcal{P}) \\ \tilde{t}_n \tilde{\lambda}_n &= \sum_{p \in \mathcal{P}} \frac{\tilde{t}_p \tilde{\lambda}_p}{\sigma_n - \sigma_p}, & (n \in \mathcal{N}). \end{aligned} \quad (24)$$

In other words,

$$\begin{aligned} \lambda_p &= \lambda(\sigma_p), & t_p &= t(\sigma_p), \\ \tilde{\lambda}_n &= \tilde{\lambda}(\sigma_n), & \tilde{t}_n &= \tilde{t}(\sigma_n), \end{aligned} \quad (25)$$

which also suggests that we should identify $\tilde{t}(\sigma)$ in (23) with $1/t(\sigma)$. These are the scattering equations used in the ambitwistor string theories [14].

Next, we impose Lorentz covariance. Since λ_i and $\tilde{\lambda}_i$ are Lorentz spinors, $\tilde{t}_p t_n / \sigma_{pn}$ in (24) must transform like a Lorentz scalar for every $n \in \mathcal{N}$ and $p \in \mathcal{P}$. Under a Lorentz transformation, $1/\sigma_{pn} \rightarrow \xi(\sigma_p) \xi(\sigma_n) / \sigma_{pn}$, hence we must have $t_n \rightarrow t_n / \xi(\sigma_n)$ and $\tilde{t}_p \rightarrow \tilde{t}_p / \xi(\sigma_p)$. These complicated transformation laws can be more easily visualized if we bundle t_n and σ_n into a spinor $\hat{\sigma}_n = (\sigma_n, 1) / t_n$, \tilde{t}_p and σ_p into another spinor $\hat{\sigma}_p = (\sigma_p, 1) / \tilde{t}_p$, then the fact that the spinor product $\hat{\sigma}_p \cdot \hat{\sigma}_n = \sigma_{pn} / t_n \tilde{t}_p \equiv (pn)$ is a Lorentz scalar suggests that the spinors $\hat{\sigma}_n$ and $\hat{\sigma}_p$ are indeed Lorentz spinors. This can be directly verified.

We have now three types of spinor products, $\langle ij \rangle$ for λ , $[ij]$ for $\tilde{\lambda}$, and $(pn) = -(np)$ for $\hat{\sigma}$.

With this notation, (23) written in the form

$$\lambda(\sigma) = \sum_{n \in \mathcal{N}} \frac{\lambda_n}{(\sigma n)}, \quad \tilde{\lambda}(\sigma) = \sum_{p \in \mathcal{P}} \frac{\tilde{\lambda}_p}{(\sigma p)}, \quad (26)$$

where $(\sigma n) = (\sigma - \sigma_n) / \tilde{t}(\sigma) t_n$, $(\sigma p) = (\sigma - \sigma_p) / t(\sigma) \tilde{t}_p$, clearly shows that $\lambda(\sigma)$ and $\tilde{\lambda}(\sigma)$ are

spinor densities of weight 0. The spinor scattering equations (24), written in the form,

$$\begin{aligned} F_p(\hat{\boldsymbol{\sigma}}) &\equiv \lambda_p - \sum_{n \in \mathcal{N}} \frac{\lambda_n}{(pn)} = 0, \\ \tilde{F}_n(\hat{\boldsymbol{\sigma}}) &\equiv \tilde{\lambda}_n - \sum_{p \in \mathcal{P}} \frac{\tilde{\lambda}_p}{(np)} = 0, \end{aligned} \quad (27)$$

tells us that the function $\phi_i(E, \boldsymbol{\sigma}, \boldsymbol{\tau})$ in (2) should now be identified with $F_p(\hat{\boldsymbol{\sigma}})$ and $\tilde{F}_n(\hat{\boldsymbol{\sigma}})$, with the auxiliary variables $\boldsymbol{\tau}$ given by t_n and t_p . The integration measure in (1) and (2) can now be combined to be $d^2\hat{\sigma}_n = d\sigma_n dt_n / t_n^3$ and $d^2\hat{\sigma}_p = d\sigma_p dt_p / t_p^3$.

C. Holographic spinor-helicity amplitude

Momentum conservation is hidden in the spinor scattering equations. Using (27) and the fact that $(pn) = -(np)$, it is easy to show that $\sum_{i=1}^n k_i = \sum_{n \in \mathcal{N}} k_n + \sum_{p \in \mathcal{P}} k_p = \sum_{n \in \mathcal{N}} \lambda_n \tilde{\lambda}_n + \sum_{p \in \mathcal{P}} \lambda_p \tilde{\lambda}_p = 0$. The amplitude in (1) and (2) are defined with the momentum-conservation factor $\delta^4(\sum_{i=1}^n k_i)$ extracted. This δ^4 -function is hidden in two $\delta^2(F_n)$ or two $\delta^2(\tilde{F}_p)$. For the sake of definiteness we will take them to be the former from now on, with $n = I, J$, and have them removed before writing the scattering amplitude M .

With all these considerations, (1) and (2) for the color-stripped gluon amplitude can now be written as

$$M_n = \int \left(\prod_{n \in \mathcal{N}, n \neq I, J} d^2\hat{\sigma}_n \delta^2(F_n(\hat{\boldsymbol{\sigma}})) \right) \left(\prod_{p \in \mathcal{P}} d^2\hat{\sigma}_p \delta^2(\tilde{F}_p(\hat{\boldsymbol{\sigma}})) \right) N_{IJ} D_n, \quad (28)$$

where N_{IJ} is a normalization factor that depends on I, J . The energy dimension $4 - n$ of the amplitude is now contained completely in the $\delta^2(F_n)$ and $\delta^2(\tilde{F}_p)$, leaving D_n dimensionless. To ensure a local interaction, we shall assume it to be momentum independent to avoid the appearance of a form factor. To maintain Lorentz invariance, we take it to be a function of $(ij) = \hat{\sigma}_i \hat{\sigma}_j$, invariant under cyclic permutation as is required for a color-stripped amplitude.

To determine D_n and N_{IJ} , we resort to the scaling relation (21).

First, examine (27). In order to keep that invariant under a scaling operation (21), we must also scale every $\hat{\sigma}_n$ and $\hat{\sigma}_p$ according to

$$\hat{\sigma}_n \rightarrow s_n \hat{\sigma}_n, \quad \hat{\sigma}_p \rightarrow \tilde{s}_p \hat{\sigma}_p. \quad (29)$$

The factor $\langle IJ \rangle^2 \prod_{n \neq I, J} \delta^2(F_n) \prod_p \delta^2(\tilde{F}_p)$ then scales exactly like M in (21). Under (29), $(IJ)^2 \prod_{n \neq I, J} d^2\hat{\sigma}_n \prod_p d^2\hat{\sigma}_p$ would also scales like M in (21), thus if we let $N_{IJ} = \langle IJ \rangle^2 (IJ)^2$,

then D_n must scale also exactly like M in (21), namely,

$$D_n \rightarrow \left(\prod_{n \in \mathcal{N}} s_n^2 \prod_{p \in \mathcal{P}} \tilde{s}_p^2 \right) D_n. \quad (30)$$

The easiest way to have a Lorentz-invariant D_n that (30), cyclic symmetry, as well as factorization is to have

$$D_n = \frac{1}{(12)(23) \cdots (n-1, n)(n1)}. \quad (31)$$

As before, adding cyclically permuted cross-ratios like $(ij)(kl)/(ik)(jl)$ would ruin factorization and therefore not allowed. Putting all these together, the spinor helicity amplitude for the color-stripped gluon amplitude is given by

$$M_n = \int \left(\prod_{n \in \mathcal{N}, n \neq I, J} d^2 \hat{\sigma}_n \delta^2(F_n(\hat{\sigma})) \right) \left(\prod_{p \in \mathcal{P}} d^2 \hat{\sigma}_p \delta^2(\tilde{F}_p(\hat{\sigma})) \right) \frac{\langle IJ \rangle^2 (IJ)^2}{(12)(23) \cdots (n1)}. \quad (32)$$

It is known that the amplitude is independent of the choice of I and J [23].

V. SCALAR LOOP AMPLITUDES

In a quantum field theory of scalar particles, any ℓ -loop diagram can be obtained from a tree diagram by folding ℓ -pairs of its off-shell lines. If q_a ($a = 1, \dots, \ell$) are the momenta of these lines, then the loop amplitude is equal to the off-shell tree amplitude, with propagators $1/(q_a^2 - m^2 + i\epsilon)$ inserted and loop momenta q_a integrated. Since we know how to write a holographic off-shell tree amplitude *with the correct propagators*, this procedure can simply be copied over to obtain a holographic expression for a scalar amplitude for any number of loops. In the language of (2), the off-shell momenta q_a can be regarded as the auxiliary variables τ .

To illustrate this operation, we shall write down the holographic representation of the 1-loop self energy diagram, whose usual field-theoretic expression in $4-\epsilon$ dimension is (Fig. 4)

$$\begin{aligned} \Sigma(k) &= \int \frac{d^{4-\epsilon} q}{(q^2 - m^2)((k+q)^2 - m^2)} = \int_0^1 d\alpha \int \frac{d^{4-\epsilon} q}{[(1-\alpha)(q^2 - m^2) + \alpha((k+q)^2 - m^2)]^2} \\ &\sim \int_0^1 d\alpha \frac{1}{\epsilon} [\alpha(1-\alpha)k^2 - m^2]^{-\epsilon}, \end{aligned} \quad (33)$$

where α is the Feynman parameter, and \sim means proportional to.

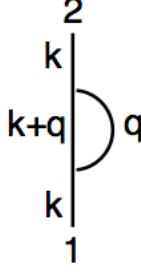


Fig. 4. One-loop self energy

As described above, the holographic 1-loop amplitude is obtained by folding two legs of a 4-point off-shell holographic tree amplitude. Choosing p, q, r of (14) to be 2,3,4, the 4-point holographic tree amplitude is given by

$$M_4 \sim \int \frac{d\sigma_1}{\hat{f}_1} \frac{1}{\sigma_{(1234)}\sigma_\beta}, \quad (34)$$

where \hat{f}_1 is given in (5) and μ_{ij} is shown in (11) and (12). For the s -channel diagram on the left of Fig. 2, $\sigma_\beta = \sigma_{(1243)}$, and for the t -channel diagram on the right of Fig. 2, $\sigma_\beta = \sigma_{(1324)}$.

To obtain the loop diagram in Fig. 4, we only require the t -channel diagram of M_4 , with $k_1 = -k_2 = k$ and $-k_3 = k_4 = q$. It is given by

$$M_4 \sim \int_{\mathcal{O}} \frac{d\sigma_1}{\hat{f}_1} \frac{(\sigma_{23}\sigma_{34}\sigma_{42})^2}{(\sigma_{12}\sigma_{23}\sigma_{34}\sigma_{41})(\sigma_{13}\sigma_{32}\sigma_{24}\sigma_{41})}, \quad (35)$$

$$\begin{aligned} \hat{f}_1 &= \frac{-m^2}{\sigma_{12}} + \frac{-2k \cdot q - k^2 - q^2 + 2m^2}{\sigma_{13}} + \frac{2k \cdot q + k^2 + q^2 - m^2}{\sigma_{14}} \\ &= \frac{m^2\sigma_{23}}{\sigma_{12}\sigma_{13}} - \frac{(2k \cdot q + k^2 + q^2 - m^2)\sigma_{34}}{\sigma_{13}\sigma_{14}}, \end{aligned} \quad (36)$$

where \mathcal{O} is a contour surrounding $\hat{f}_1 = 0$. To show that this integral does yield the correct t -channel diagram given by $1/((k+q)^2 - m^2)$, we distort the contour \mathcal{O} away from $\hat{f}_1 = 0$ to surround the poles of C_4 instead. Now C_4 contains poles at $\sigma_{12} = 0, \sigma_{13} = 0$ and $\sigma_{14} = 0$, but \hat{f}_1 also contains simple poles at these locations. The only way for the integrand of (35) to contain a simple pole is to have a double pole present at C_4 , and this occurs only at $\sigma_{14} = 0$. The contribution from this pole to the integral is

$$M_4 \sim \frac{1}{2k \cdot q + k^2 + q^2 - m^2} = \frac{1}{(k+q)^2 - m^2},$$

which is the right result.

Substituting this holographic expression M_4 for the t -channel propagator into (33), we get the holographic representation of the 1-loop self energy amplitude to be

$$\Sigma(k) = \int \frac{d^{4-\epsilon}q M_4}{(q^2 - m^2)} \sim \int \frac{d^{4-\epsilon}q}{(q^2 - m^2)} \int_{\mathcal{O}} \frac{d\sigma_1}{\hat{f}_1} \frac{(\sigma_{23}\sigma_{34}\sigma_{42})^2}{(\sigma_{12}\sigma_{23}\sigma_{34}\sigma_{41})(\sigma_{13}\sigma_{32}\sigma_{24}\sigma_{41})}. \quad (37)$$

The result is of course identical to (33).

If one wants, (37) can be cast in the form of (1) and (2), with $n = 2$. There are now $m = 6$ auxiliary variables, σ_3, σ_4 , and the q^α . There are $n + x = 4$ scattering equations, $\hat{f}_1 = 0$ and three others fixing the values of $\sigma_2, \sigma_3, \sigma_4$. One can also introduce the Feynman parameter α to combine the quadratic q -dependences in the denominator, and then carry out the q -integration. The result is to replace the $m = 6$ auxiliary variables by $m = 3$: σ_2, σ_3 , and α .

ACKNOWLEDGMENTS

I am grateful to James Bjorken, Bo Feng, Song He, Yu-tin Huang, Chia-Hsien Shen, and York-Peng Yao for interesting discussions.

-
- [1] S. Parke and T. Taylor, Phys. Rev. Lett. **56** (1986) 2459.
 - [2] R. Britto, F. Cachazo, B. Feng, E. Witten, Phys. Rev. Lett. **94** (2005) 181602 [arXiv: hep-th/0501052].
 - [3] H. Elvang and Y.-t. Huang, ‘Scattering Amplitudes in Gauge Theory and Gravity’, Cambridge University Press 2015 [arXiv:1308.1697].
 - [4] E. Witten, Commun.Math.Phys. **252** (2004)189 [arXiv: hep/th-0312171].
 - [5] R.Penrose, J. Math. Phys. **8** (1967) 345.
 - [6] R. Roiban, M. Spradlin, A. Volovich, Phys. Rev. D **70** (2004) 026009 [arXiv:hep-th/0403190]; N. Arkani-Hamed, F. Cachazo, C. Cheung, J. Kaplan, JHEP **03** (2010) 110 [arXiv:0903.2110]; JHEP **03** (2010) 020 [arXiv:0907.5418]; N. Arkani-Hamed, F. Cachazo, C. Cheung, JHEP **03** (2010) 036 [arXiv:0909.0483]; Louise Dolan, Peter Goddard, JHEP **0912** (2009) 032 [arXiv:0909.0499v2]; F. Cachazo, arXiv:1301.3970.
 - [7] F. Cachazo, S. He, and E.Y. Yuan, Phys. Rev. D **90** (2014) 065001 [arXiv: 1306.6575].

- [8] F. Cachazo, S. He, and E.Y. Yuan, Phys. Rev. Lett. **113** (2014) 17161 [arXiv: 1307.2199].
- [9] F. Cachazo, S. He, and E.Y. Yuan, JHEP **1407** (2014) 033 [arXiv: 1309.0885].
- [10] F. Cachazo, S. He, and E.Y. Yuan, JHEP **1501** (2015)121 [arXiv: 1409.8256].
- [11] F. Cachazo, S. He, and E.Y. Yuan, JHEP **1507** (2015) 149 [arXiv:1412.3479].
- [12] T. Adamo, E. Casali, D. Skinner, JHEP **04** (2014) 104 [arXiv:1312.3828]; Y. Geyer, L. Mason, R. Monteiro, P. Tourkine, Phys. Rev. Lett. **115** (2015) 121603 [arXiv:1507.00321]; C. Baadsgaard, N.E.J. Bjerrum-Bohr, J.L. Bourjaily, P.H. Damgaard, B. Feng, JHEP 1511 (2015) 080 [arXiv:1508.03627]; S. He, E.Y. Yuan, Phys. Rev. D **92** (2015) 105004 [arXiv:1508.06027]; M. Yu, C. Zhang, Y-Z. Zhang, JHEP **06** (2017) 051 [arXiv:1704.01290];
- [13] L. Mason, D. Skinner, JHEP **07** (2014) 048 [arXiv:1311.2564]; N. Berkovits, JHEP **03** (2014) 017 [arXiv:1311.4156v2]; N. E. J. Bjerrum-Bohr, P. H. Damgaard, P. Tourkine, P. Vanhove, Phys. Rev. **D90** (2014) 106002 [arXiv: 1403.4553]; E. Casali, Y. Geyer, L. Mason, R. Monteiro, K.A. Roehrig, JHEP **11** (2015) 038 [arXiv:1506.08771]; W. Siegel, arXiv:1512.02569; Eduardo Casali, Piotr Tourkine, JHEP **11** (2016) 036 [arXiv:1606.05636]; Y. Geyer, arXiv:1610.04525; Y. Li, W. Siegel, arXiv:1702.07332.
- [14] Y. Geyer, A.E. Lipstein, L.J. Mason, Phys. Rev. Lett. **113** (2014) 081602 [arXiv:1404.6219].
- [15] J. de Boer, S.N. Solodukhin, Nucl. Phys. **B665** (2003) 545 [arXiv: hep-th/0303006]; D. Kapec, P. Mitra, A.-M. Raclariu, A. Strominger, Phys. Rev. Lett. **119** (2017) 121601 [arXiv:1609.00282]; C. Cheung, A. de la Fuente, R. Sundrum, JHEP **01** (2017) 112 [arXiv:1609.00732]; C. Cardona, Y-t. Huang, JHEP **08** (2017) 133 [arXiv:1702.03283]; S. Pasterski, S-H. Shao, A. Strominger, arXiv:1706.03917.
- [16] S.G. Naculich, JHEP **09** (2014) 029 [arXiv:1407.7836].
- [17] S.G. Naculich, JHEP **05** (2015) 050 [arXiv:1501.03500].
- [18] B. Feng, JHEP **05** (2016) 061 [arXiv:1601.05864].
- [19] C.S. Lam and Y-P. Yao, Nucl. Phys. **B907** (2016) 678 [arXiv:1511.05050].
- [20] C.S. Lam and Y-P. Yao, Phys. Rev. D **93** (2016) 105004 [arXiv:1512.05387].
- [21] C.S. Lam and Y-P. Yao, Phys. Rev. D **93** (2016)105008 [arXiv:1602.06419].
- [22] S. He, Z. Liu, J-B. Wu, JHEP **07** (2016) 060 [arXiv:1604.02834].
- [23] F. Cachazo, Y. Geyer, arXiv:1206.6511.